J. Fluid Mech. (1971), *vol.* 48, *part* 4, *pp.* 673–688
Printed in Great Britain

The Rayleigh problem for a slightly diffusive density-stratified fluid

By R. G. STANDING

Department of the Mechanics of Fluids,
University of Manchester

(Received 17 August 1970 and in revised form 14 March 1971)

A doubly-infinite sloping flat plate, initially at rest in a slightly diffusive viscous density-stratified fluid, starts to move impulsively with a constant velocity along the line of greatest slope. The resulting flow is found to be an unsteady motion superimposed on a steady diffusion-induced flow, which is present throughout. Laplace transform methods give solutions which are valid either in an essentially non-diffusive outer layer or in a diffusive inner layer. The impulsive start sets up oscillations in the outer layer. These gradually die out, and a steady diffusive flow develops.

A glass plate was towed vertically through stratified brine, into which aluminium particles were introduced. The flow velocities deduced from the particle motions confirmed the theoretical predictions.

1. Introduction

This simple problem illustrates some of the physical processes which affect transient and oscillatory viscous boundary-layer flows on bodies moving slowly through density-stratified fluids. It shows how molecular diffusion affects the flow when the diffusion coefficient is small.

Existing work on boundary-layer flows in viscous density-stratified fluids includes several studies of steady two-dimensional boundary layers on a horizontal finite flat plate. Martin & Long (1968) and Pao (1968) obtained similarity solutions which describe the flow near the plate and in its upstream wake when the diffusion coefficient is small. Pao also presented flow velocity profiles obtained experimentally. Brown (1968) used a Wiener-Hopf technique to obtain a solution valid near the leading and trailing edges of the plate. Kelly & Redekopp (1970) investigated the conditions under which an upstream wake flow occurs; otherwise there is a Blasius type of flow with no upstream influence. Redekopp (1970) discussed the effects of molecular and thermal diffusion.

Dore (1969) used Laplace transform methods to study the flow generated when an initially stationary vertical flat plate starts to oscillate at a constant frequency in a viscous non-diffusive density-stratified fluid. He obtained the Laplace transform of the flow velocity, described an appropriate inversion contour, and obtained the periodic solution valid at large times.

The Rayleigh problem in a density-stratified fluid is solved here by using Laplace transform and matching techniques. The undisturbed fluid has a

constant stable vertical density gradient produced by varying the solute concentration. A doubly-infinite sloping flat plate, initially at rest in the fluid, starts to move impulsively with a constant velocity U along the line of greatest slope. The resulting flow is seen to be an unsteady motion, in which fluid velocities are proportional to U, superimposed on a steady diffusion-induced flow of the type discussed by Wunsch (1970) and Phillips (1970). There can be no state of rest in a stratified fluid above a sloping infinite plate. Even when the plate is at rest a slow steady flow maintains the zero normal density gradient at the plate.

The inverse Schmidt number ϵ is usually very small in a fluid which is stratified by a gradient of solute concentration. In such a fluid, where $\epsilon \ll 1$, molecular diffusion affects the motion in a thin layer close to the plate. The solution may be expanded as a series in powers of $\epsilon^{\frac{1}{2}}$ in an essentially non-diffusive outer layer. By neglecting powers of $\epsilon^{\frac{1}{2}}$ above the lowest, and terms exponentially small when $\epsilon \ll 1$, an outer non-diffusive solution is found. The exponentially small terms behave singularly in a thin inner layer, where an inner diffusive solution is found. The impulsive start sets up oscillations in the outer layer, which gradually die out. A steady flow develops, in which molecular diffusion disperses solute convected with the plate, and viscous and buoyancy forces alone determine the motion.

A glass plate was towed vertically through a tank of stably-stratified brine with a constant density gradient. The results of this experiment are presented in §5. Fluid motions were deduced from the movement of aluminium dust in suspension in the tank. Measured flow velocities and displacements compared favourably with the theoretical predictions.

2. The equations of motion

The positive x and y directions are taken along and at right angles to the line of greatest slope of a doubly-infinite sloping flat plate, and make angles α and $\alpha - \frac{1}{2}\pi$ respectively with the upwards vertical (figure 1). The half-space $y > 0$ is filled with an incompressible fluid, whose undisturbed background density is

$$\rho_0 = \bar{\rho} - Kx\cos\alpha - Ky\sin\alpha,$$

where $\bar{\rho}$ is the density at the origin of the co-ordinates, and $K > 0$ is the undisturbed vertical density gradient, assumed to be constant. The fluid velocity $\mathbf{q}$ has components u and v in the x and y directions respectively, and time t is measured from the impulsive start at $t = 0$. Variations in solute concentration c are small enough to ensure that ν, the kinematic viscosity, and $\mathscr{D}$, the molecular diffusivity, are constant. The equations of motion are

$$\frac{D\mathbf{q}}{Dt} = -\frac{1}{\rho}\nabla p - \mathbf{g} + \nu\nabla^2\mathbf{q},$$

$$Dc/Dt = \mathscr{D}\nabla^2 c,$$

$$\nabla . \mathbf{q} = 0,$$

where ρ is the fluid density, p is the pressure, $D/Dt = (\partial/\partial t) + u(\partial/\partial x) + v(\partial/\partial y)$, and

$\nabla^2 = \partial^2/\partial x^2 + \partial^2/\partial y^2$. The density of the fluid is assumed to depend linearly on the concentration of solute:

$$\rho = \bar{\rho}(1+\gamma c),$$

where γ is a constant. It is assumed that the Boussinesq approximation is valid, and that the stratification scale height L and $\cos\alpha$ are large enough (condition (2.5)) to make the flow one-dimensional. Then $\mathbf{q}$ and $\rho - \rho_0$ are independent of x, $v = 0$ and $\partial p/\partial x = -\rho_0 g \cos\alpha$. The equations of motion become

$$\left.\begin{aligned} \frac{\partial u}{\partial t} &= -\frac{fg\cos\alpha}{\bar{\rho}} + \nu\frac{\partial^2 u}{\partial y^2}, \\ \frac{\partial f}{\partial t} &= Ku\cos\alpha + \mathscr{D}\frac{\partial^2 f}{\partial y^2}, \end{aligned}\right\} \tag{2.1}$$

where $f = \rho - \rho_0$. Equations (2.1) also describe the flow set up by a flat plate which starts to oscillate at a constant frequency (Dore 1969).

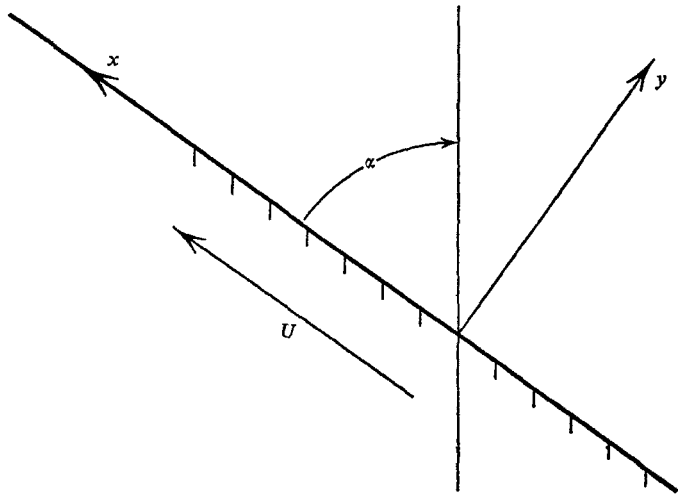

FIGURE 1. The co-ordinate system for flow over an infinite sloping flat plate.

No solute can cross the plane $y = 0$; thus

$$\partial c/\partial y = 0 \quad \text{at} \quad y = 0.$$

Also

$$(\rho - \rho_0) \to 0, \quad u \to 0 \quad \text{as} \quad y \to \infty.$$

These conditions may be written

$$\left.\begin{aligned} &\partial f/\partial y = K\sin\alpha \quad \text{at} \quad y = 0 \quad \text{for all } t, \\ &f \to 0, \quad u \to 0 \quad \text{as} \quad y \to \infty \quad \text{for all } t. \end{aligned}\right\} \tag{2.2a}$$

The impulsive start provides further conditions at $y = 0$:

$$u = 0 \quad \text{for} \quad t < 0, \quad u = U \quad \text{for} \quad t > 0. \tag{2.2b}$$

When $\cos\alpha \neq 0$ the equations may be transformed as follows. Dimensionless variables are defined by

$$t' = \omega_0 t\cos\alpha, \quad y' = y\left(\frac{\omega_0\cos\alpha}{\nu}\right)^{\frac{1}{2}},$$
$$u' = u/U, \qquad f' = \omega_0 f/KU,$$

where the Brunt–Väisälä frequency $\omega_0 = (Kg/\bar{\rho})^{\frac{1}{2}}$. From now on dimensionless quantities only are of interest, and the dashes are omitted. Equations (2.1) become

$$\left.\begin{aligned}\frac{\partial u}{\partial t} &= -f + \frac{\partial^2 u}{\partial y^2},\\ \frac{\partial f}{\partial t} &= u + \epsilon\frac{\partial^2 f}{\partial y^2},\end{aligned}\right\} \tag{2.3}$$

where $\epsilon = \mathscr{D}/\nu$. Boundary conditions (2.2) become

$$\left.\begin{aligned}\frac{\partial f}{\partial y} = \frac{\sin\alpha}{U}\left(\frac{\omega_0\nu}{\cos\alpha}\right)^{\frac{1}{2}} \quad &\text{at} \quad y = 0 \quad \text{for all } t,\\ f\to 0, \quad u\to 0 \quad &\text{as} \quad y\to\infty \quad \text{for all } t,\\ u = 0 \quad \text{for} \quad t < 0, \quad u = 1, \quad &\text{for} \quad t > 0 \quad \text{at} \quad y = 0.\end{aligned}\right\} \tag{2.4}$$

When $\cos\alpha$ is small some additional terms must be retained in the equations of motion. The flow may be treated as one-dimensional provided

$$\cos\alpha \gg (\epsilon Ra)^{-\frac{1}{2}}, \tag{2.5}$$

where $Ra = \omega_0^2 L^4/\nu\epsilon$ is the Rayleigh number, and L is the stratification scale height of the fluid (cf. Wunsch 1970). In practice Ra is often very large. In the experiments described in §5 the Rayleigh number was of order 10^{18}. The theory is valid until the plate is almost, but not quite, horizontal.

3. The steady diffusion induced flow

Wunsch (1970) and Phillips (1970) showed that there can be no state of rest in a stratified fluid above a sloping infinite plate. When the plate is at rest there is a flow in which convection and diffusion maintain the zero normal density gradient at the wall.

New variables are defined by

$$Y = \epsilon^{-\frac{1}{4}}y, \quad u_0 = \eta^{-1}u, \quad f_0 = \eta^{-1}\epsilon^{\frac{1}{2}}f,$$

where

$$\eta = \frac{\sin\alpha}{U}\left(\frac{\nu\epsilon^{\frac{3}{2}}\omega_0}{\cos\alpha}\right)^{\frac{1}{2}}.$$

In a steady state equations (2.3) become

$$-f_0 + \frac{d^2u_0}{dY^2} = 0, \quad u_0 + \frac{d^2f_0}{dY^2} = 0.$$

At times $t < 0$ the plate is at rest. Conditions (2.4) for $t < 0$ become

$$df_0/dY = 1, \quad u_0 = 0 \quad \text{at} \quad Y = 0,$$
$$f_0\to 0, \quad u_0\to 0 \quad \text{as} \quad Y\to\infty.$$

The steady solution, found by Wunsch and Phillips, is

$$\left.\begin{aligned} u_0 &= 2^{\frac{1}{2}} e^{-Y/2^{\frac{3}{2}}} \sin Y/2^{\frac{1}{2}}, \\ f_0 &= -2^{\frac{1}{2}} e^{-Y/2^{\frac{3}{2}}} \cos Y/2^{\frac{1}{2}}. \end{aligned}\right\} \tag{3.1}$$

This solution, which also describes the steady stratified flow over a heated sloping flat plate, is due to Prandtl (1952, p. 422), and is also relevant to other thermal convection problems, such as the flow in a vertical slot (Elder 1965; Gill 1966). The Veronis (1967) analogy shows that this solution also describes the steady flow on a heated vertical wall in a rotating fluid (Barcilon & Pedlosky 1967).

The complete solution of the Rayleigh problem may be regarded as a superposition of two solutions,

$$\left.\begin{aligned} u &= \eta u_0 + u^*, \\ f &= \eta \epsilon^{-\frac{1}{2}} f_0 + f^*, \end{aligned}\right\} \tag{3.2}$$

where u^* and f^* are the solutions of (2.3) that satisfy the initial and boundary conditions

$$\left.\begin{aligned} u^* = f^* = 0 \quad &\text{for all } y \quad \text{for} \quad t < 0, \\ u^* = 1, \quad \partial f^*/\partial y = 0 \quad &\text{for} \quad t > 0, \\ u^* \to 0, \quad f^* \to 0 \quad &\text{as} \quad y \to \infty \quad \text{for} \quad t > 0. \end{aligned}\right\} \tag{3.3}$$

In practice the diffusion-induced velocity component is usually very small; typical velocities would be of the order of 10^{-3} to 10^{-2} mm/s in the stratified salt solution described in §5. If $\eta \ll 1$ the component ηu_0 may be neglected in comparison with u^*. In particular when $\alpha = 0$ the Rayleigh problem has the solution $u = u^*$ and $f = f^*$. Phillips (1970) pointed out that in a thermally stratified fluid the velocities induced by thermal diffusion would be much larger, and in a fluid with a stable thermal stratification and a very small Prandtl number, such as mercury, the velocity could be large enough to generate turbulent flow.

4. The superimposed unsteady flow

Veronis (1967) showed that there is an analogy between many stratified and rotating flow systems. The present problem has a rotating unstratified flow analogue when $\epsilon = 1$. Singh & Sathi (1968) obtained the solution for the flow over an impulsively started horizontal flat plate in an unstratified rotating fluid. The stratified analogue of their solution satisfies equations (2.3) with $\epsilon = 1$, and all but one of conditions (3.3); this condition specifies $f^* = 0$ at $y = 0$ instead of $\partial f^*/\partial y = 0$ at $y = 0$. The Singh & Sathi solution is a simple combination of error and exponential functions, but the zero mass flux condition at the plate gives a more complex solution.

The solutions u^* and f^* are uniformly valid throughout the (y, t) plane for any value of ϵ, however small. Laplace transforms will be denoted by a bar:

$$\bar{\psi} = \int_0^\infty \psi e^{-st} dt,$$

where in this case ψ denotes u^* or f^*. These satisfy transformed equations (2.3) and conditions (3.3), so that

$$\bar{u}^* = [n_2(n_2^2 - s)\,e^{-n_1 y} - n_1(n_1^2 - s)\,e^{-n_2 y}]/hs,$$
$$\bar{f}^* = (n_2 e^{-n_1 y} - n_1 e^{-n_2 y})/\epsilon hs,$$

where n_1 and n_2 are the roots of

$$\epsilon n^4 - sn^2(1+\epsilon) + (1+s^2) = 0$$

which have positive real parts, and

$$h = (n_2 - n_1)\,(n_2^2 + n_1 n_2 + n_1^2 - s).$$

The inverse transforms of $\bar{u}^*$ and $\bar{f}^*$ may be obtained by means of an integration around a suitable contour in the complex s plane.

When $\epsilon \ll 1$ molecular diffusion affects the flow in a thin layer close to the plate only. The solutions in the outer non-diffusive and inner diffusive layers may be obtained by taking appropriate limits for $\bar{u}^*$ and $\bar{f}^*$ as $\epsilon \to 0$. The following matching method is used here instead. In the essentially non-diffusive outer layer the solution may be expanded as a series:

$$\bar{u}^* = \sum_{n=0}^{\infty} \left(a_n \exp\left\{ -y\left(s + \frac{1}{s}\right)^{\frac{1}{2}} \right\} + c_n \exp\left\{ -y\left(\frac{s}{\epsilon}\right)^{\frac{1}{2}} \right\} \right) \epsilon^{\frac{1}{2}n},$$
$$\bar{f}^* = \sum_{n=0}^{\infty} \left(b_n \exp\left\{ -y\left(s + \frac{1}{s}\right)^{\frac{1}{2}} \right\} + d_n \exp\left\{ -y\left(\frac{s}{\epsilon}\right)^{\frac{1}{2}} \right\} \right) \epsilon^{\frac{1}{2}n}.$$

This outer layer is represented as region 1 in figure 2, where $y/t^{\frac{1}{2}} = O(1)$ and $t = O(1)$. If powers of $\epsilon^{\frac{1}{2}}$ above the lowest, and terms exponentially small when $\epsilon \ll 1$ are neglected, the lowest-order solution satisfies equations (2.3) with the diffusion term omitted. But the neglected exponential terms become significant in a layer $y/t^{\frac{1}{2}} = O(\epsilon^{\frac{1}{2}})$ close to the plate, however small ϵ is. This diffusive layer

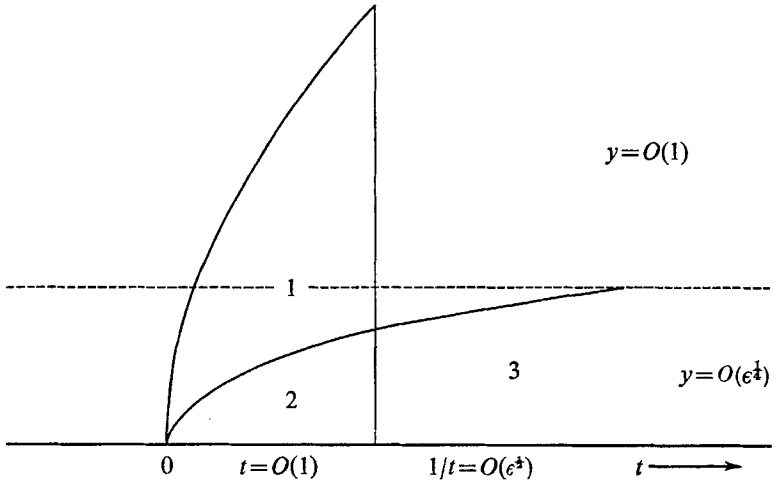

FIGURE 2. The flow layer structure. Region 1, the non-diffusive layer $y/t^{\frac{1}{2}} = O(1)$, $t = O(1)$; region 2, the diffusive layer $y/t^{\frac{1}{2}} = O(\epsilon^{\frac{1}{2}})$, $t = O(1)$; region 3, the diffusive layer $y/t^{\frac{1}{2}} = O(\epsilon^{\frac{1}{2}})$, $1/t = O(\epsilon^{\frac{1}{2}})$. The layer $y = O(\epsilon^{\frac{1}{2}})$, where the diffusion-induced flow occurs, is bounded by the dotted line.

consists of the two regions numbered 2 and 3 in figure 2, where $t = O(1)$ and $1/t = O(\epsilon^{\frac{1}{2}})$ respectively. Outside these three regions the solution is trivial: $u^* = 0$ and $f^* = 0$. The lowest-order terms in the expansions of u^* and f^* in each region i are denoted by u_i and f_i, where i takes the value 1, 2 or 3. These terms are matched (Van Dyke 1964, ch. 5) at the boundaries between adjacent regions. No higher-order terms in the expansions are considered, as the lowest-order terms appear to show all the essential features of the motion.

In figure 2 the region $y = O(\epsilon^{\frac{1}{4}})$, between the dotted line and the plate, represents the layer affected by the steady diffusion-induced flow.

4.1. *The outer non-diffusive region* 1: $y/t^{\frac{1}{2}} = O(1)$, $t = O(1)$

When $y/t^{\frac{1}{2}} = O(1)$ the diffusion term in equations (2.3) may be neglected, but since the neglected term is a second-order derivative, the solution of the reduced equations cannot satisfy all of conditions (3.3). The zero solute flux condition, associated with the diffusion process, is omitted. The lowest-order terms u_1 and f_1 in the expansions of u^* and f^* in region 1 satisfy

$$\partial u_1/\partial t = -f_1 + (\partial^2 u_1/\partial y^2), \quad \partial f_1/\partial t = u_1,$$

and conditions (3.3) reduce to

$$\begin{aligned} &u_1 = f_1 = 0 \quad \text{for all } y \quad \text{for} \quad t < 0, \\ &u_1 = 1 \quad \text{at} \quad y = 0 \quad \text{for} \quad t > 0, \\ &u_1 \to 0, \quad f_1 \to 0 \quad \text{as} \quad y \to \infty \quad \text{for} \quad t > 0. \end{aligned}$$

The Laplace transforms of u_1 and f_1 are

$$\bar{u}_1 = \frac{1}{s}\exp\left\{-y\left(s+\frac{1}{s}\right)^{\frac{1}{2}}\right\} \quad \text{and} \quad \bar{f}_1 = \frac{1}{s^2}\exp\left\{-y\left(s+\frac{1}{s}\right)^{\frac{1}{2}}\right\},$$

and the inverse transforms (Erdelyi *et al.* 1954) are

$$\left.\begin{aligned} u_1 &= \int_0^t J_0[2(t\tau-\tau^2)^{\frac{1}{2}}]\phi(\tau)\,d\tau, \\ f_1 &= \int_0^t \left(\frac{t}{\tau}-1\right)^{\frac{1}{2}} J_1[2(t\tau-\tau^2)^{\frac{1}{2}}]\phi(\tau)\,d\tau, \end{aligned}\right\} \tag{4.1}$$

where $\phi(\tau) = \frac{1}{2}y(\pi\tau^3)^{-\frac{1}{2}}\exp(-y^2/4\tau)$, and J_0 and J_1 are Bessel functions of order zero and one respectively.

When t is small, $J_0[2(t\tau-\tau^2)^{\frac{1}{2}}] \simeq 1$, so that $u_1 \simeq \operatorname{erfc}(y/2t^{\frac{1}{2}})$. This is the solution of the Rayleigh problem when the fluid is unstratified.

The integrals u_1 and f_1 were evaluated numerically, and are shown in figure 3 as functions of t at $y = 0{\cdot}8, 1{\cdot}1, 1{\cdot}6$ and 3. The zero-velocity contour in the (y, t) plane, shown in figure 4(*a*), divides the plane into regions of up- and downflow. Immediately after the start fluid at all distances from the plate is convected with it through the action of viscous forces. Before $t = 0{\cdot}5$ buoyancy forces have induced a reverse flow for all $y > 1{\cdot}4$. The flow pattern thereafter consists of a region of upflow close to the plate and reverse flow further out. On this is superimposed a slowly decaying oscillation with a period of 2π. For $y > 2$ the contour

sections in figure 4(*a*) are almost horizontal: the motion there is almost entirely oscillatory.

Since $u_1 = \partial f_1/\partial t$ the fluid displacement d_1 is equal to f_1. When u_1 is zero, d_1 is either a maximum or minimum. These maximum and minimum values of d_1 as functions of y are shown in figure 4(*b*). The curve changes direction twice near $y = 0{\cdot}8$. This corresponds to the kink in the zero-velocity contour in figure 4(*a*). The cluster of curves at the right-hand side of figure 4(*b*) corresponds to the oscillations for $y > 2$. For clarity all except the first oscillation have been omitted.

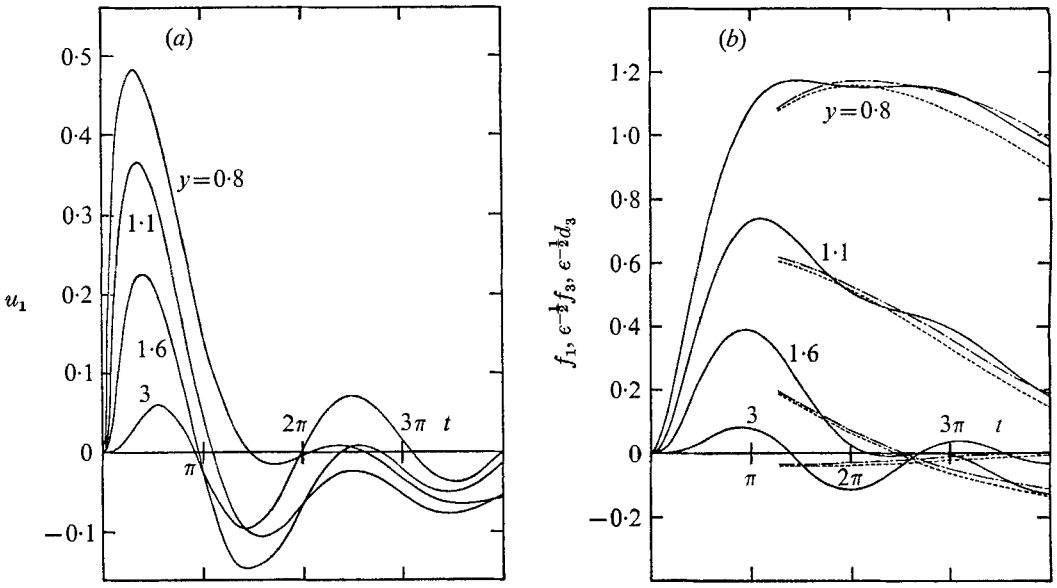

FIGURE 3. The time-variation of (*a*) the velocity u_1; (*b*) ——, the density f_1; –·–, the density $\epsilon^{-\frac{1}{2}}f_3$; – – –, the fluid displacement $\epsilon^{-\frac{1}{2}}d_3$, at $y = 0{\cdot}8$, 1·1, 1·6 and 3. $\epsilon = 1{\cdot}2 \times 10^{-3}$.

The development of the shear, $(-\partial u_1/\partial y)_{y=0}$, with time is shown in figure 5. The shear decreases initially like the corresponding unstratified flow wall shear. As the reverse flow develops near $t = 1$, the shear starts to increase and tends to infinity asymptotically like $2(t/\pi)^{\frac{1}{2}}$.

4.2. *The inner diffusive region* 2: $y/t^{\frac{1}{2}} = O(\epsilon^{\frac{1}{2}})$, $t = O(1)$

The molecular diffusion term in equation (2.3) must be retained in the region $y/t^{\frac{1}{2}} = O(\epsilon^{\frac{1}{2}})$. In region 2 define $Y' = \epsilon^{-\frac{1}{2}}y$. Then u^* and f^* satisfy the transformed equations (2.3),

$$\epsilon\,\partial u^*/\partial t = -\epsilon f^* + (\partial^2 u^*/\partial Y'^2),$$

$$\partial f^*/\partial t = u^* + (\partial^2 f^*/\partial Y'^2).$$

Ignoring terms of order ϵ, the lowest-order solutions u_2 and f_2 in region 2 satisfy the reduced equations

$$\partial^2 u_2/\partial Y'^2 = 0, \quad \partial f_2/\partial t = u_2 + (\partial^2 f_2/\partial Y'^2),$$

subject to the conditions

$$u_2 = 1, \quad \partial f_2/\partial Y' = 0 \quad \text{at} \quad Y' = 0,$$

and the matching conditions at the region 1 boundary

$$u_2 \sim 1, \quad f_2 \sim t \quad \text{as} \quad Y'/t^{\frac{1}{2}} \to \infty.$$

Solutions satisfying these conditions are

$$u_2 = 1, \quad f_2 = t. \tag{4.2}$$

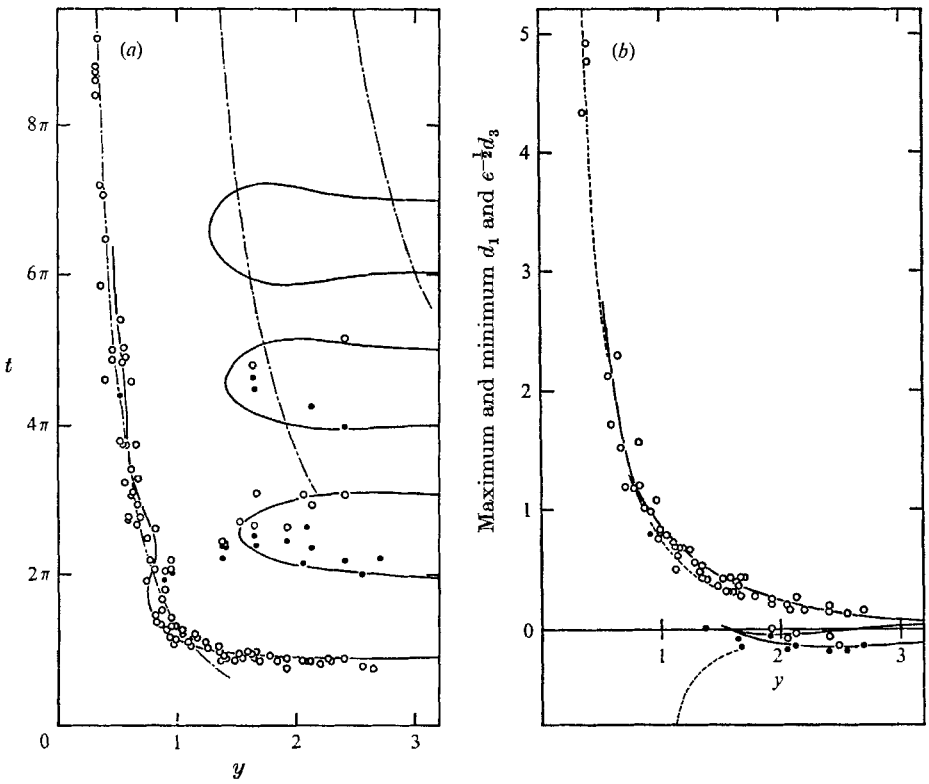

FIGURE 4. (*a*) The zero velocity contour: ——, zero u_1; –·–, zero u_3. (*b*) Maximum and minimum displacements: ——, maximum or minimum d_1; – – –, maximum or minimum $\epsilon^{-\frac{1}{2}}d_3$. $\epsilon = 1{\cdot}2 \times 10^{-3}$. Experimental points: ○, maximum fluid displacement; ●, minimum fluid displacement, both in the direction of the plate motion.

4.3. *The subsequent flow pattern. Region* 3: $y/t^{\frac{1}{2}} = O(\epsilon^{\frac{1}{2}}), 1/t = O(\epsilon^{\frac{1}{2}})$

New variables are defined by

$$T = \epsilon^{\frac{1}{2}}t, \quad Y = \epsilon^{-\frac{1}{4}}y.$$

Equations (2.3) become

$$\epsilon(\partial u^*/\partial T) = -\epsilon^{\frac{1}{2}}f^* + (\partial^2 u^*/\partial Y^2),$$
$$\epsilon^{\frac{1}{2}}(\partial f^*/\partial T) = u^* + \epsilon^{\frac{1}{2}}(\partial^2 f^*/\partial Y^2).$$

Since $f_2 = t, f^* = O(\epsilon^{-\frac{1}{2}})$ in region 3. Thus the lowest-order terms u_3 and $\epsilon^{-\frac{1}{2}}f_3$, in expansions of u^* and f^* in region 3, satisfy the reduced equations

$$0 = -f_3 + (\partial^2 u_3/\partial Y^2), \quad \partial f_3/\partial T = u_3 + (\partial^2 f_3/\partial Y^2);$$

and conditions (3.3) become

$$u_3 = 1, \quad \partial f_3/\partial Y = 0 \quad \text{at} \quad Y = 0,$$
$$u_3 \to 0, \quad f_3 \to 0 \quad \text{as} \quad Y \to \infty.$$

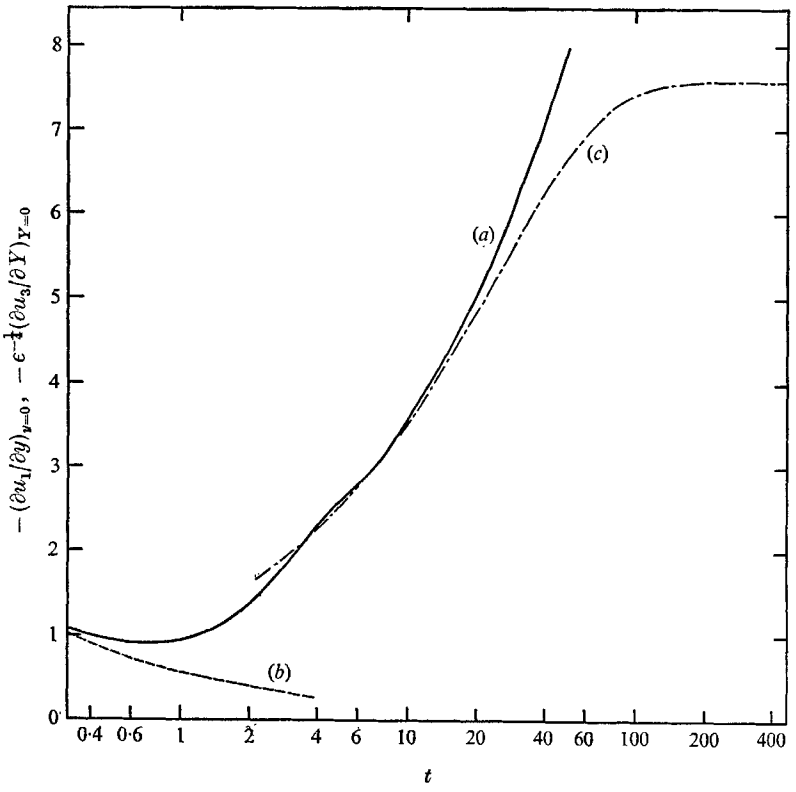

FIGURE 5. The wall shear. (*a*) $-(\partial u_1/\partial y)_{y=0}$; (*b*) the wall shear when the fluid is unstratified; (*c*) $-\epsilon^{-\frac{1}{2}}(\partial u_3/\partial Y)_{Y=0}$. $\epsilon = 1{\cdot}2 \times 10^{-3}$.

The solution must be matched with the region 2 solution, so that

$$u_3 \sim 1, \quad f_3 \sim T \quad \text{as} \quad T \to 0. \tag{4.3}$$

The Laplace transforms of u_3 and f_3, defined by

$$\bar{u}_3 = \int_0^\infty u_3 e^{-ST}\,dT \quad \text{and} \quad \bar{f}_3 = \int_0^\infty f_3 e^{-ST}\,dT,$$

are

$$\bar{u}_3 = \frac{1}{S} e^{-S_1 Y}\left\{\cos S_2 Y + \frac{S-1}{S+1}\frac{S_1}{S_2}\sin S_2 Y\right\}$$

and

$$\bar{f}_3 = \frac{1}{S(S+1)} e^{-S_1 Y}\left\{\cos S_2 Y + \frac{S_1}{S_2}\sin S_2 Y\right\},$$

where $S_1 = \frac{1}{2}(2+S)^{\frac{1}{2}}$ and $S_2 = \frac{1}{2}(2-S)^{\frac{1}{2}}$. The inverse transforms are represented formally by the Bromwich integrals

$$u_3 = \frac{1}{2\pi i}\int_{\beta-i\infty}^{\beta+i\infty} \bar{u}_3 e^{ST}\,dS \quad \text{and} \quad f_3 = \frac{1}{2\pi i}\int_{\beta-i\infty}^{\beta+i\infty} \bar{f}_3 e^{ST}\,dS.$$

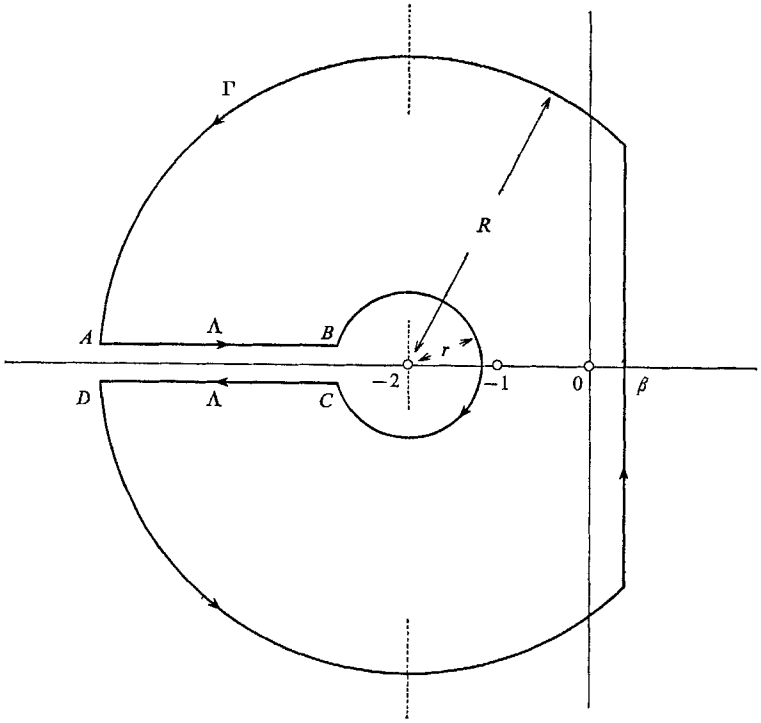

FIGURE 6. The contour of integration, Γ.

These were evaluated by means of an integration around the closed contour Γ shown in figure 6. Both $\bar{u}_3$ and $\bar{f}_3$ have simple poles at $S = 0$ and -1 in the complex S plane, and a branch point at $S = -2$. The integrals around the contour Γ,

$$u_\Gamma = \frac{1}{2\pi i}\int_\Gamma \bar{u}_3 e^{ST}\,dS \quad \text{and} \quad f_\Gamma = \frac{1}{2\pi i}\int_\Gamma \bar{f}_3 e^{ST}\,dS,$$

are given by the residues at the poles at $S = 0$ and -1:

$$\left.\begin{aligned} u_\Gamma &= \left(\cos\frac{Y}{2^{\frac{1}{2}}} - \sin\frac{Y}{2^{\frac{1}{2}}}\right)\exp\left(-\frac{Y}{2^{\frac{1}{2}}}\right) + \frac{2}{3^{\frac{1}{2}}}\sin\frac{3^{\frac{1}{2}}Y}{2}\exp\left(-\frac{Y}{2} - T\right), \\ f_\Gamma &= \left(\cos\frac{Y}{2^{\frac{1}{2}}} + \sin\frac{Y}{2^{\frac{1}{2}}}\right)\exp\left(-\frac{Y}{2^{\frac{1}{2}}}\right) - \left(\cos\frac{3^{\frac{1}{2}}Y}{2} + \frac{1}{3^{\frac{1}{2}}}\sin\frac{3^{\frac{1}{2}}Y}{2}\right)\exp\left(-\frac{Y}{2} - T\right). \end{aligned}\right\} \tag{4.4}$$

The contributions to u_Γ and f_Γ from integrals around the small circle of radius r and the large circle of radius R, with centres at $S = -2$, tend to zero as $r \to 0$

and $R \to \infty$. In the same limits, as $r \to 0$ and $R \to \infty$, the contributions to u_Γ and f_Γ from the integrals along Λ, the straight lines AB and CD, become u_Λ and f_Λ where

$$\left.\begin{aligned} u_\Lambda &= \frac{1}{\pi}\int_0^\infty \frac{e^{-(\xi+2)T}}{\xi+2}\left\{\sin\eta_1\cos\eta_2 - \frac{\xi+3}{\xi+1}\left(\frac{\xi}{\xi+4}\right)^{\frac{1}{2}}\cos\eta_1\sin\eta_2\right\}d\xi, \\ f_\Lambda &= \frac{1}{\pi}\int_0^\infty \frac{e^{-(\xi+2)T}}{(\xi+1)(\xi+2)}\left\{\left(\frac{\xi}{\xi+4}\right)^{\frac{1}{2}}\cos\eta_1\sin\eta_2 - \sin\eta_1\cos\eta_2\right\}d\xi, \end{aligned}\right\} \tag{4.5}$$

where $\eta_1 = \frac{1}{2}Y\xi^{\frac{1}{2}}$ and $\eta_2 = \frac{1}{2}Y(4+\xi)^{\frac{1}{2}}$. Then u_3 and f_3 are given by

$$u_3 = u_\Gamma - u_\Lambda \quad \text{and} \quad f_3 = f_\Gamma - f_\Lambda.$$

The integral contributions (4.5) decay at least as fast as e^{-2T}, while u_Γ and f_Γ consist of two parts: one decays as e^{-T}, the other is the eventual steady-state solution $u_\infty(Y)$ and $f_\infty(Y)$.

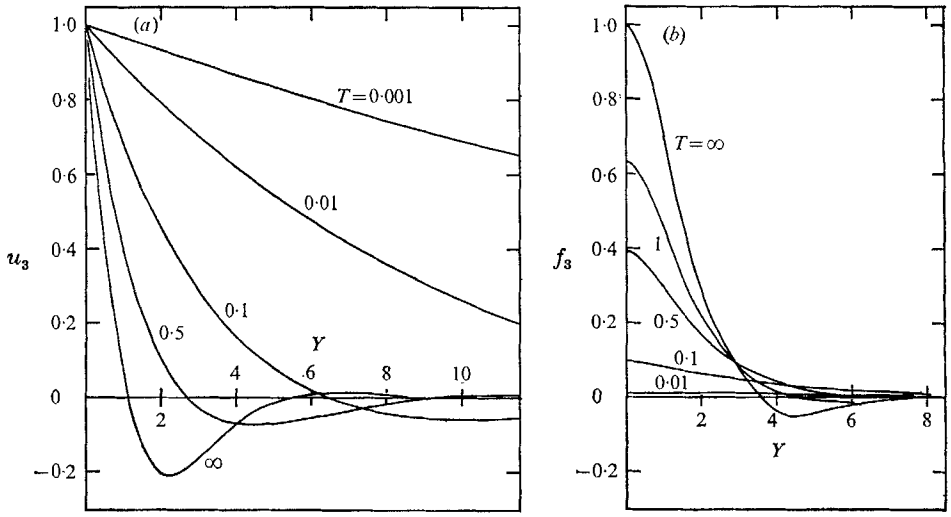

FIGURE 7. (*a*) The velocity profile $u_3(Y)$; (*b*) the density profile $f_3(Y)$, at T = 0·001, 0·01, 0·1, 0·5, 1 and ∞.

The integrals u_Λ and f_Λ were evaluated numerically, and profiles of u_3 and f_3 are shown in figure 7 at T = 0·001, 0·01, 0·1, 0·5, 1 and ∞. The matching condition (4.3) is satisfied: $u_3 \to 1$ and $f_3 \to 0$ as $T \to 0$. As T increases from zero a reverse flow region develops and moves towards the plate; further regions of up- and downflow appear, and the flow tends towards the steady state represented by the $T = \infty$ profiles. The fluid displacement d_3 is defined by

$$d_3 = \int_0^T u_3 dT.$$

When $T < 1$ the solute concentration is only slightly affected by molecular diffusion. The d_3 and f_3 profiles are almost coincident, so that separate d_3 profiles are not shown. But the density gradients gradually steepen, and molecular

diffusion increasingly affects the solute concentration in the flow layer, so that d_3 and f_3 diverge. In the limit, as $T \to \infty$, f_3 tends to a constant value while d_3 tends to infinity.

It is of interest to compare the region 1 and region 3 solutions on the same time and length scales. For this purpose the particular value of ϵ chosen was

$$\epsilon = 1{\cdot}2 \times 10^{-3},$$

a value appropriate to the diffusion of salt in water under the experimental conditions described in §5. In figure 3(*b*) $\epsilon^{-\frac{1}{2}} f_3$ and $\epsilon^{-\frac{1}{2}} d_3$ are compared with f_1, equal to d_1, at $y = 0{\cdot}8$, 1·1, 1·6 and 3. Corresponding curves lie close together, and

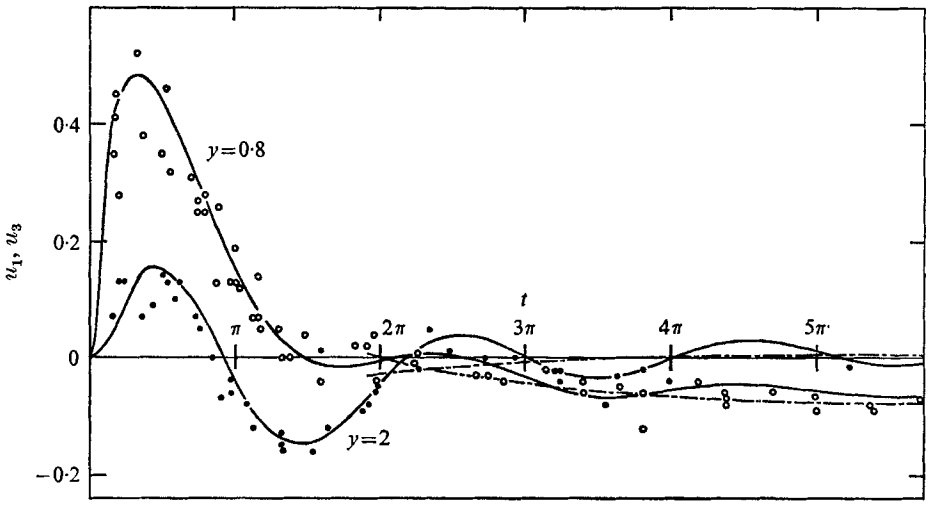

FIGURE 8. The time-variation of: ——, u_1; –·–, u_3, at $y = 0{\cdot}8$ and 2. $\epsilon = 1{\cdot}2 \times 10^{-3}$. Experimental points: ○, $0{\cdot}75 < y < 0{\cdot}85$; ●, $1{\cdot}9 < y < 2{\cdot}1$.

it appears that $\epsilon^{-\frac{1}{2}} f_3$ represents a 'mean' value about which f_1 oscillates. Corresponding values of u_1 and u_3 at $y = 0{\cdot}8$ and 2 are shown in figure 8. When $5 < t < 20$ the contours of zero u_1 and u_3, shown in figure 4(*a*), are almost coincident close to the plate. Further from the plate the oscillatory part of u_1 is at least as large as u_3, and the contours are unrelated. The maximum and minimum values of d_1 and $\epsilon^{-\frac{1}{2}} d_3$, which are associated with the zeros of u_1 and u_3, and are shown in figure 4(*b*), are almost equal close to the plate, but are more widely separated away from the plate and at later times. Diffusion affects the motion only after a considerable time.

The unsteady contribution to the wall shear $-\epsilon^{-\frac{1}{4}}(\partial u_3/\partial Y)_{Y=0}$, shown in figure 5, tends towards a constant value $2^{\frac{1}{2}}\epsilon^{-\frac{1}{4}}$ as $T \to \infty$. When $4 < t < 40$ the solutions valid in regions 1 and 3 give almost identical values of the wall shear. Thus even close to the wall, where diffusion effects are expected to be most apparent, diffusion does not seriously affect the shear at least until $t = 20$.

5. Experiments

A glass-sided tank, which was 160 cm long, 90 cm high and 55 cm from front to back, was filled with a stratified salt solution having a constant density gradient. Mowbray (1967) described how the tank was filled. A vertical glass plate spanned the tank from front to back, and was immersed in the fluid with its upper edge above the free surface and attached to a towing device. The plate was towed upwards at various speeds between 0·2 and 1·6 mm/s. It could travel up to 25 cm, guided by vertical rails mounted inside the tank at the centre of the front and back faces. The flow layer was at most 2–3 mm thick. Observations were made at least 15 cm below the free surface, 5 cm from the front glass wall, and 5 cm above the lower edge of the plate. These distances seemed to be sufficient to eliminate wall, surface and trailing edge effects, and only slight deviations from one-dimensional flow were seen. These small transverse motions were probably more apparent than real, resulting from refractive index variations in the fluid.

Aluminium dust in suspension was introduced into the tank at the surface about 6 h before experiments were due to start. During this period heavy particles sank to the bottom, leaving particles, small compared with the flow layer thickness, falling at about 10^{-2} mm/s. Flow velocities were obtained by subtracting the average particle fall velocity immediately before the impulsive start from subsequent measured particle velocities. The inertial velocities of particles relative to the fluid were probably very much smaller and were neglected. A ciné camera attached to a long-focal-length microscope was used to record particle motions for subsequent analysis. The distance from each particle to the plate was obtained by halving the apparent distance between the particle and its reflexion in the glass surface of the plate.

The dimensionless parameter $U^2/\nu\omega_0$ took values between 0·03 and 2, and ϵ was approximately $1{\cdot}2 \times 10^{-3}$. The Boussinesq approximation, assumed in §2, remained valid during the experiments, and density variations never became comparable with $\bar{\rho}$. The relative density variation in the eventual steady state, which was of the order of $KU/(\omega_0 \bar{\rho} \epsilon^{\frac{1}{2}})$, never exceeded 10^{-2}. All measurements of times, distances and velocities were made dimensionless for comparison with the theoretical values.

In figure 8 experimental values of the fluid velocity at $y = 0{\cdot}8$ and 2 are presented, together with the two theoretical solutions u_1 and u_3. The experimental velocities are scattered, partly because they could not be measured instantaneously, and the transition from one solution to the other in the range $6 < t < 20$, where u_1 and u_3 are close, is not clearly shown. Points of zero velocity are shown in figure 4 (*a*), and the maximum or minimum displacements associated with these zeros are shown in figure 4 (*b*). The position, time and displacement associated with the first velocity zero compare favourably with the theoretical values. During the second and third oscillation fluid velocities were small, but zeros appear at least within the right region of the (y, t) plane.

The last graph, figure 9, shows the steady-state velocity profile, which developed about 60 s after the start of one particular run. Refractive index variations in the fluid seriously affected measurements of the particle-to-plate distance

at this stage of the motion, because density gradients were at their steepest. Particles appeared to be closer to the plate than they were. The dotted curve in figure 9 is the expected apparent position of the theoretical velocity profile, as seen by an observer outside the tank. Known values of U, ω_0 and ϵ for that run were used, and refractive index variations were assumed to depend linearly on a density given by $f_3 = f_\infty(Y)$. A light path equation given by Rossi (1959, p. 56) was integrated numerically through the flow layer to give mean apparent positions of a particle and its reflexion in the plate, and hence the apparent particle-to-plate distance. During the early stages of each run this apparent particle displacement was small, and has been neglected.

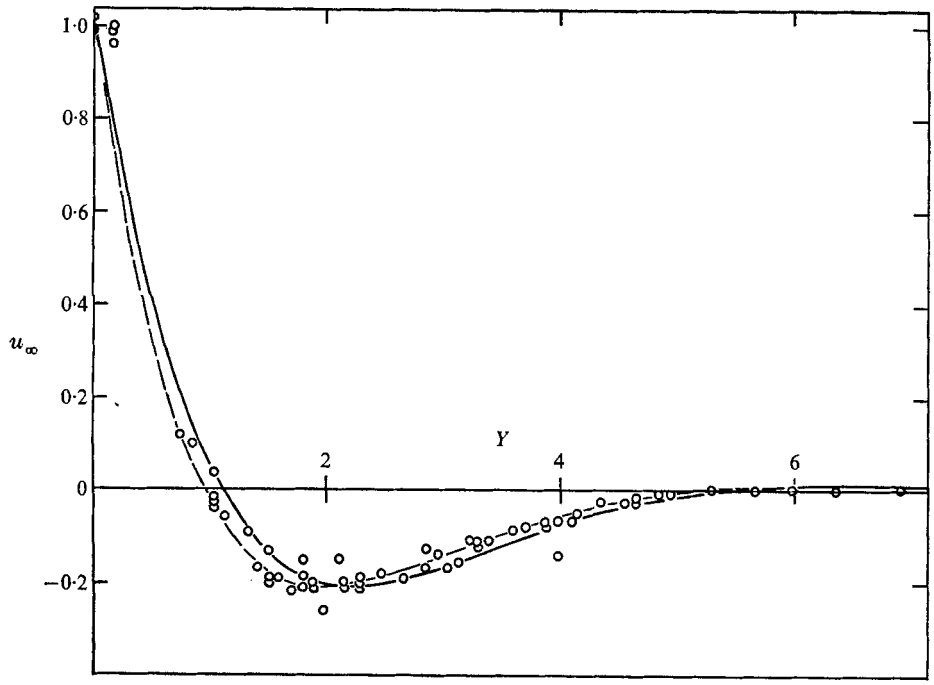

FIGURE 9. ——, the steady velocity profile $u_\infty(Y)$; – – –, the expected apparent position of $u_\infty(Y)$ because of refractive index variations. ○, experimental points.

6. Conclusion

A slow steady diffusion-induced flow occurs on a sloping flat plate at rest in a density-stratified fluid. The impulsive start of the plate sets up oscillations in an outer non-diffusive viscous flow layer at the natural frequency, $\omega_0 \cos\alpha$, of fluid particle oscillations at an angle α to the vertical. These oscillations die out slowly through viscous action. After a time $O(\epsilon^{\frac{1}{2}}\omega_0 \cos\alpha)^{-1}$ a steady flow develops in a diffusive layer of thickness $O([\nu\epsilon^{\frac{1}{2}}/(\omega_0 \cos\alpha)]^{\frac{1}{2}})$. In this layer convection and diffusion maintain the steady density distribution, and viscous and buoyancy forces maintain the flow.

Phillips (1970) mentioned an experimental situation where a few of these results may be applied. When he inserted a flat plate into a tank of stratified salt

solution, where ω_0 was about 4 rad/s, he noticed that the transient motions died away within a few seconds. Suppose that a laminar steady flow, of the type described in §4.3, developed before the plate came to rest. The solution describing the flow past an impulsively stopped plate is simply the difference between the initial steady solution and the unsteady contribution to the solution describing the flow past an impulsively started plate. Thus transient motions should have died away in a time of order $(\epsilon^{\frac{1}{2}}\omega_0)^{-1}$, or less than 10 s after the plate came to rest.

I should like to thank Dr T. N. Stevenson for supervising this work, and Dr J. A. King-Hele for several helpful discussions. Acknowledgement is made to the Science Research Council for a maintenance grant. Dr Stevenson conducted the experiments, supported by the Ministry of Technology.

REFERENCES

BARCILON, V. & PEDLOSKY, J. 1967 Linear theory of rotating stratified fluid motions. *J. Fluid Mech.* **29**, 1–16.

BROWN, S. 1968 Viscous flow of a stratified fluid past a finite flat plate. *Proc. Roy. Soc.* A **306**, 239–256.

DORE, B. D. 1969 Forced vertical oscillations in a viscous stratified fluid. *Proc. Camb. Phil. Soc.* **66**, 617–627.

ELDER, J. W. 1965 Laminar free convection in a vertical slot. *J. Fluid Mech.* **23**, 77–98.

ERDELYI, A., MAGNUS, W., OBERHETTINGER, F. & TRICOMI, F. G. 1954 *Tables of Integral Transforms*, vol. 1. Bateman Manuscript Project. McGraw-Hill.

GILL, A. E. 1966 The boundary layer régime for convection in a rectangular cavity. *J. Fluid Mech.* **26**, 515–536.

KELLY, R. E. & REDEKOPP, L. G. 1970 The development of horizontal boundary layers in stratified flow. Part 1. Non-diffusive flow. *J. Fluid Mech.* **42**, 497–512.

MARTIN, S. & LONG, R. R. 1968 The slow motion of a flat plate in a viscous stratified fluid. *J. Fluid Mech.* **31**, 669–688.

MOWBRAY, D. E. 1967 The use of schlieren and shadowgraph techniques in the study of flow patterns in density stratified liquids. *J. Fluid Mech.* **27**, 595–608.

PAO, Y. H. 1968 Laminar flow of a stably stratified fluid past a flat plate. *J. Fluid Mech.* **34**, 795–808.

PHILLIPS, O. M. 1970 On flows induced by diffusion in a stably stratified fluid. *Deep-Sea Res.* **17**, 435–443.

PRANDTL, L. 1952 *Essentials of Fluid Dynamics*. Blackie.

REDEKOPP, L. G. 1970 The development of horizontal boundary layers in stratified flow. Part 2. Diffusive flow. *J. Fluid Mech.* **42**, 513–526.

ROSSI, B. 1959 *Optics*. Addison-Wesley.

SINGH, M. P. & SATHI, H. L. 1968 An exact solution in rotating flow. *J. Maths. Mech.* **18**, 193–200.

VAN DYKE, M. 1964 *Perturbation Methods in Fluid Mechanics*. Academic.

VERONIS, G. 1967 Analogous behaviour of homogeneous, rotating fluids and stratified, non-rotating fluids. *Tellus*, **19**, 326–336.

WUNSCH, C. 1970 On oceanic boundary mixing. *Deep-Sea Res.* **17**, 293–301.